CHEMISTRY
A EUROPEAN JOURNAL

Bis(oxofluorenediyl)oxacyclophanes: Synthesis, Crystal Structure and Complexation with Paraquat in the Gas Phase

Nikolay G. Lukyanenko,*[a] Tatiana I. Kirichenko,[a] Alexander Yu Lyapunov,[a] Alexander V. Mazepa,[a] Yurii A. Simonov,[b] Marina S. Fonari,[b] and Mark M. Botoshansky[c]

Abstract: The first three representatives of the new family of oxacyclophanes incorporating two 2,7-dioxyfluorenone fragments, connected by $[\text{-}CH_2CH_2O\text{-}]_m$ spacers ($m=2$–4), have been synthesized. The yield of the smallest oxacyclophane ($m=2$) is considerably higher with respect to the larger ones ($m=3$ and $m=4$), which are formed in comparable yields. Molecular modeling and NMR spectra analysis of the model compounds suggest that an essential difference in oxacyclophanes yields is caused by formation of quasi-cyclic intermediates, which are preorganized for macrocyclization owing to intramolecular π–π stacking interactions between the fluorenone units. The solid-state structures of these oxacyclophanes exhibit intra- and intermolecular π–π stacking interactions that dictate their rectangular shape in the fluorenone backbone and crystal packing of the molecules with the parallel or T-shape arrangement. The crystal packing in all cases is also sustained by weak C–H···O hydrogen bonds. FAB mass spectral analysis of mixtures of the larger oxacyclophanes ($m=3$ and $m=4$) and a paraquat moiety revealed peaks corresponding to the loss of one and two PF_6^- counterions from the 1:1 complexes formed. However, no signals were observed for complexes of the paraquat moiety with the smaller oxacyclophane ($m=2$). Computer molecular modeling of complexes revealed a pseudorotaxane-like incorporation of the paraquat unit, sandwiched within a macrocyclic cavity between the almost parallel-aligned fluorenone rings of the larger oxacyclophanes ($m=3$ and $m=4$). In contrast to this, only external complexes of the smallest oxacyclophane ($m=2$) with a paraquat unit have been found in the energy window of 10 kcal mol^{-1}.

Keywords: crown compounds · cyclophanes · fluorenones · host–guest systems · macrocycles

Introduction

In the design and synthesis of new molecular receptors, cyclophanes play an important role as versatile host compounds that are capable of entrapping molecular guests within the central cavity or sandwiching them between host molecules in the crystal lattice.[1] Host compounds are commonly designed by using rigid building blocks in order to stabilize a hollow ring conformation. Recently, oxacyclophane-type macrocycles incorporating rigid aromatic moieties bridged by flexible polyethers chains have attracted considerable attention. Such compounds successfully couple properties of classical crown ethers and cyclophanes. This feature makes them excellent receptors both for ionic and neutral guests.[2]

As a powerful recognition tool utilized to guide the complexation and the synthesis of supramolecular species, various types of noncovalent intermolecular interactions can be used. These are, specifically, hydrogen bonds, stacking, elec-

[a] Prof. N. G. Lukyanenko, Dr. T. I. Kirichenko, A. Y. Lyapunov, Dr. A. V. Mazepa
Department of Fine Organic Synthesis
A. V. Bogatsky Physico-Chemical Institute
National Academy of Sciences of Ukraine
Lustdorfskaya doroga 86, 65080 Odessa (Ukraine)
Fax: (+38) 482-340-803, (+38) 482-652-012
E-mail: ngl@farlep.net

[b] Dr. Y. A. Simonov, Dr. M. S. Fonari
Institute of Applied Physics Academy of Sciences of Moldova
Academy str., 5 MD 2028, Chisinau (Moldova)

[c] Dr. M. M. Botoshansky
Department of Chemistry
Technion—Israel Institute of Technology
Technion City, 32000 Haifa (Israel)

Supporting information for this article is available on the WWW under http://www.chemeurj.org/ or from the author.

DOI: 10.1002/chem.200400870

trostatic, hydrophobic, and charge-transfer interactions, as well as metal coordination.[3] Nevertheless, the electrostatic interactions play a dominant role, and in the case in which polar subsystems are included into the macrocyclic host framework, it is possible to identify the total stabilization energy within the limits of the electrostatic energy term.[4] Therefore, the introduction of extended aromatic moieties containing polar groups and well-developed, polarized π-electron systems into the framework of macrocyclic hosts seems a reasonable approach to enhance such interactions. Most of the investigations in this direction are based on the synthesis of polar receptors that contain appropriately positioned hydroxy or carboxy groups in a rigid macrocyclic framework.[1b,5] The other polar groups, especially the carbonyl groups, can serve as hydrogen-bond acceptors and play an essential role in the determination of the binding ability of the hosts, the three-dimensional chemical structure, and the properties of their complexes.

One of the most significant advances in the field of supramolecular chemistry resulted from the quest for effective hosts for the complexation of 1,1′-dialkyl-4,4′-bipyridinium salts (paraquats). During the 1980s Stoddart et al.[6] discovered that large bisarylene crown ethers, in particular, combine into pseudorotaxanes (mechanically threaded structures without bulky end groups) with paraquat units with association constants about 10^2–$10^3\,M^{-1}$.[6] This research initiated the synthesis of a variety of pseudorotaxanes, rotaxanes, catenanes, and polyrotaxanes.[7]

The structure of bisarylene crown ethers is similar to the framework of oxacyclophanes, since each of them contains rigid aromatic moieties bridged by flexible polyethers chains. Therfore, their complexing ability should also be similar. In addition, it is apparent that the binding ability of the oxacyclophanes that contain polar groups can be appreciably augmented by attractive electrostatic interactions between the macrocyclic host and the positively charged guest.

With the purpose of obtaining the macrocyclic receptors that potentially possess high intrinsic affinity to electron-deficient guests, we were interested in 2,7-dioxy-9*H*-fluoren-9-one (**1**)[8] as an aromatic block for synthesis of new family of large oxacyclophanes namely bis(oxofluorenediyl)oxacyclophanes. Bisphenol **1** was selected for the following reasons:

1) It is a highly polarized π-electron-rich extended aromatic system, in which the carbonyl group can act as a sensor that recognizes an electron-deficient guest, can direct it towards the macrocyclic host cavity and can stabilize the complexes because of electrostatic interactions.
2) It is a powerful hydrogen-bond acceptor; the carbonyl oxygen atom is capable to form strong hydrogen bonds with the substrate, which is often the dominating factor in molecular recognition and self-assembly of supramolecular systems.
3) Fluorenone and its derivatives have good luminescence properties that are important for the development of sensitive fluorescence-based chemosensors.
4) Finally, the carbonyl group of the fluorenone fragment can be converted into a variety of functional groups; this allows for finetuning of the binding behavior of the oxacyclophanes.

In a preliminary communication, we discussed briefly the preparation and some structural features of oxacyclophane **12**.[9] Here we report: 1) the preparation of the first three representatives of the bis(oxofluorenediyl)oxacyclophanes, 2) the X-ray structural analysis of the oxacyclophanes, and 3) the complexation of the oxacyclophanes with 1,1′-dimethyl-4,4′-bipyridinium bis(hexafluorophosphate) (paraquat) in the gas phase.

Results and Discussion

Synthesis: The synthetic pathway leading to the oxacyclophanes **11–13** is shown in Scheme 1. Reaction of bisphenol **1** with the chlorohydrins of di-, tri-, or tetraethylene glycol in DMF in the presence of anhydrous potassium carbonate at 80–85 °C for 40 h afforded the diols **5–7**, respectively. Conversion of these diols into bistosylates **8–10** was achieved in good yields (70–88 %) by using *p*-toluenesulfonyl chloride in

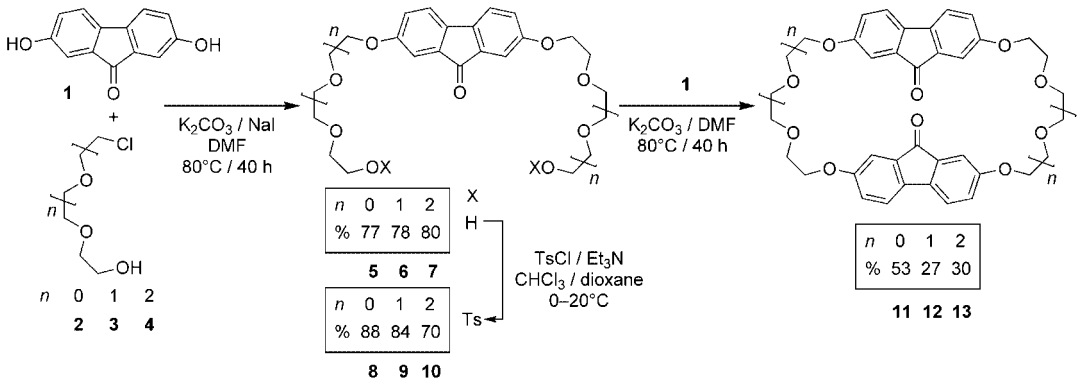

Scheme 1. Synthesis of the bis(oxofluorenediyl)oxacyclophanes **11–13**.

a mixture of chloroform and dioxane in the presence of triethylamine at 0–20 °C. Further macrocyclization reaction of the obtained bistosylates with bisphenol **1** in DMF in the presence of anhydrous potassium carbonate as the base at 80–85 °C for 40 h, under high dilution conditions, gave after workup and chromatographic purification over silica gel, the oxacyclophanes **11**–**13** in 53, 27, and 30 % yields, respectively. We did not gain any appreciable increase in yields of bis(oxofluorenediyl)oxacyclophanes by using cesium carbonate as the base instead of potassium carbonate, despite the fact that the cesium cation promotes formation of many macrocyclic systems (cesium effect).[10]

The yield of the oxacyclophane **11** is much higher with respect to oxacyclophanes **12** and **13**, which are formed in comparable yields. To find out why the yields of oxacyclophanes differ so considerably, an extensive Monte Carlo conformational search for the imaginary model compounds **14**–**16** (Figure 1) was performed with the MMFF force field

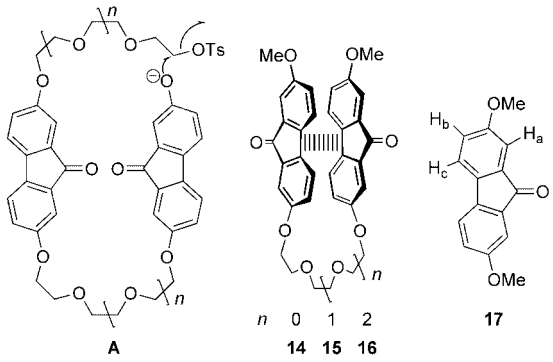

Figure 1. Schematic representation of the intermediate **A** and chemical formulas of the model compounds **14**–**17**.

as implemented in the Spartan 02 program package.[11] It resulted in minimal energy conformations of these compounds, which in all cases have an almost parallel arrangement of the partially overlapping fluorenone moieties with the interplanar distances between them equal to 3.66–3.69 Å. This geometry is commensurate with conventional parallel π–π stacking interactions between the aromatic units that stabilize a minimal energy conformations of the compounds **14**–**16**.[3d] We can therefore assume that the essential difference in the yields of the oxacyclophanes **11**–**13** is caused by the formation of the quasi-cyclic intermediate (**A**), which is preorganized for macrocyclization owing to the intramolecular π–π stacking interactions between the fluorenone units (Figure 1). According to the entropic criterion, the probability of such self-organizing should be more for molecules with the shortest length of the bridge connecting two fragments of a fluorenone. The increase in bridge length and, hence, degrees of freedom of a molecule makes formation of an intermediate (**A**) less entropically favorable, owing to restriction of internal mobility of a molecule. This is apparently the cause of the lower yields of the oxacyclophanes **12** and **13** relative to that of oxacyclophane **11**. In an effort to obtain experimental evidence of this assumption we have synthesized acyclic compounds **15** and **17** (Figure 1). As shown in Table 1, all the fluorenone proton signals in the ^{1}H NMR spectra are subject to a slight, but noticeable upfield shifts (0.02–0.06 ppm) in comparison with

Table 1. Selected ^{1}H NMR spectroscopic data[a] [δ[b] and $\Delta\delta$[c] values in ppm] for the oxacyclophanes **11**–**13** and the model compounds **15** and **17** in [D_6]DMSO at 298 K.

	Ha[d]		Hb[d]		Hc[d]	
	δ	$\Delta\delta$	δ	$\Delta\delta$	δ	$\Delta\delta$
11	6.66	−0.39	6.85	−0.16	7.17	−0.31
12	6.78	−0.27	6.80	−0.21	7.11	−0.37
13	6.84	−0.21	6.84	−0.17	7.18	−0.30
15[e]	7.12	−0.04	6.92	−0.02	7.23	−0.06
17	7.05		7.01		7.48	
17[e]	7.16		6.94		7.29	

[a] ^{1}H NMR spectra were recorded at 300 MHz. [b] The values reported correspond to the centroids of the multiplets. [c] $\Delta\delta$ values were obtained as the difference between chemical shifts of the appropriate protons of the reference compound **17** and the compounds **11**–**13**, and **15**. [d] The protons mentioned are depicted on the structural formula in Figure 1. [e] In $CDCl_3$.

those of **17**; this shift undoubtedly arises from the mutual shielding effect of the fluorenone components (Table 1). Such shielding effect reveals an appreciable population in solution of the conformation of compound **15** in which two fluorenone fragments are closely located with almost parallel alignment (shown in Figure 1). This is in a fairly good agreement with the hypotheses made about the geometry of intermediate **A**.

In solution, oxacyclophanes conformations coexist in a dynamic equilibrium, with relative populations determined by their respective energies. Since the ^{1}H NMR spectra of **11**–**13** in [D_6]DMSO show only a single set of proton signals, fast conformational exchange on the NMR timescale is taking place in the solutions of these compounds. A Monte Carlo conformational search (MMFF force field, Spartan 02) indicates that the most stable conformers of oxacyclophanes **11**–**13** are the *anti* and *syn* forms, differing in the mutual orientation of the carbonyl groups (Figure 2). Insig-

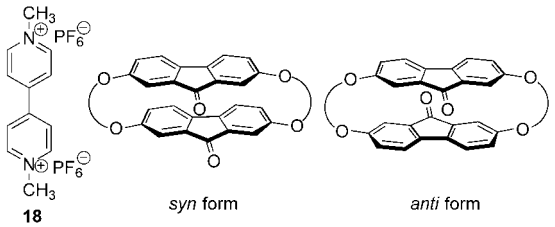

Figure 2. Chemical formula of the paraquat **18** and schematic representation of the *syn*- and *anti*-forms of the oxacyclophanes **11**–**13**.

nificant energy differences between these conformers, 0.01, 0.10, and 0.48 kcal mol^{-1} for **11**, **12**, and **13**, respectively, infer that they are almost equally populated, at least in vacuo. Analysis of CPK molecular models indicates that

these conformers can be interconverted at rotation of the fluorenone units around their long axis. The calculated (HF/3-21G*) energy barrier associated with this dynamic process in the oxacyclophane **11**, for example, is only 9 kcal mol^{-1}. Comparison of the ^{1}H NMR spectra of **11**–**13** with that of the model compound **17** indicates significant upfield shifts ($\Delta\delta$ lies between -0.16 and -0.39 ppm) for all aromatic protons (Table 1); these shifts are a result of the shielding effects exerted by the fluorenone units. This reveals that in the averaged conformations of oxacyclophanes **11**–**13** in solution, the fluorenone units are predominantly parallel and closely located, as observed in the calculated and solid-state structures.

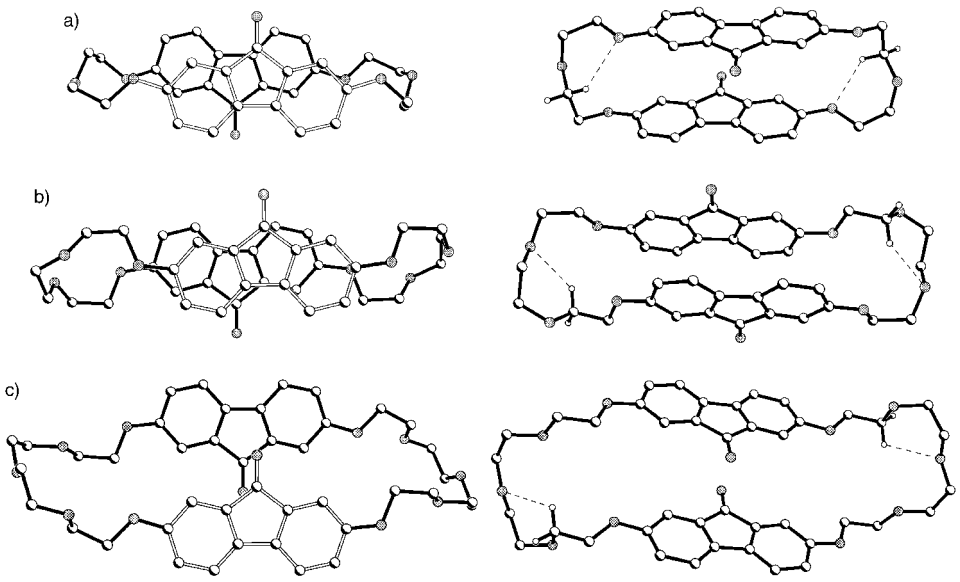

Figure 3. Top view (left) and side view (right) for the solid-state structure of the oxacyclophanes a) **11**, b) **12**, and c) **13**. There are C–H···O hydrogen bonds between the CH_2 groups and proximal oxygen atoms of the polyether loops. Their respective geometries are C···O, H···O, CH···O, 3.12, 2.45 Å, 125° for **11**; 3.17, 2.41 Å, 134° for **12**; and 3.00, 2.51 Å, 111° for **13**.

X-ray crystallography: The cavity size, the shape, the rigidity, the nature of the binding sites and intra- and intermolecular interactions govern the binding power of a host. To investigate these parameters, crystal structures of the oxacyclophanes have been studied. Single crystals suitable for X-ray crystallography were grown by crystallization of compound **11** from nitrobenzene or by slow concentration of the solutions of oxacyclophanes **12** and **13** in acetonitrile and dioxane, respectively. In all cases the initial concentrations of **11**–**13** were in the range 10^{-4}–10^{-5} M, because of their very low solubility. The molecular geometry of oxacyclophanes and their packing in the crystal are stabilized by the combination of intra- and intermolecular C–H···O hydrogen-bonding, π–π stacking interactions between the fluorenone units, and C–H···π interactions between the appropriately oriented hydrogen atoms of the methylene groups and the π-electron-rich aromatic moieties. The oxacyclophanes studied have crystallographic centers of symmetry located in the center of macrocycles owing to an antiparallel arrangement of the fluorenone units (Figure 3). Their planarity is extended to include three oxygen atoms attached to the aromatic moiety (one carbonyl group oxygen atom and two ether ones). The fused aromatic rings of the fluorenone backbone form a practically planar system. The macrocycles are self-filling, with two fluorenone units aligned parallel to each other about the crystallographic center of symmetry. The fluorenone backbone, with the distance of 9.62 Å between two attached ether oxygen atoms, dictates the rectangular shape of the macrocycle **11**, while **12** and **13** have S-shaped structures. The fluorenone units are positioned at interplanar distances of 3.53 Å in **11** and 3.45 Å in **12**; these distances correspond to the intramolecular π–π stacking interactions between them.[3] However, the corresponding fluorenone–fluorenone separation of 3.08 Å in **13** clearly indicates the absence of the intramolecular π–π stacking. In compounds **11** and **12**, the overlap of the aromatic systems is immediately apparent, being approximately the same in the both molecules (Figure 3, left column). A similar molecular shape has been found in the macrocycles that incorporate hydroquinol,[12] or biphenyl units bridged by the oxyethylene chains of the same length,[13] while in the case of the anthracene backbone the elongated shape of the molecule is distorted.[14] In compound **13**, the parallel arrangement of the fluorenone units is retained; however, one of them is considerably displaced with respect to the other in order to optimize the dipole–dipole interactions between the carbonyl groups. The oxacyclophane **13** exists in the crystals with a sigmoid edge profile reminiscent of that in bis(5-carbomethoxy-1,3-phenylene)[32]crown-10 in which the aromatic rings are parallel, but do not overlap spatially.[15] The common feature of **11**–**13** is the availability of two weak inversion-related intramolecular C–H···O interactions between the CH_2 groups and proximal oxygen atoms of the polyether loops (Figure 3, right column). The corresponding C···O separations range from 3.00 to 3.17 Å and are responsible for the formation of two intramolecular six-membered pseudorings. The short C–H···O intramolecular interactions that are found to fill the cavity are typical for classic crown ethers, although in the case of [18]crown-6 and its derivatives they act across the cavity and define the elongated shape of the molecule.[16] The oxacyclophanes **11**–**13** have centrosymmetric C_i conformations, described by an appropriate sequences of torsion angles of the crown ether loops.[17] The crystal packing in **11**–**13** is dictated by weak intermolecular C–H···O hydrogen bonds and π–π stacking in-

teractions that obey $P\bar{1}$ symmetry in **11** and **13** and $P2_1/c$ symmetry in **12** (Figure 4). The molecules of **11** and **13** are packed in a similar way into thick layers in which the surfaces are formed by the aromatic fluorenone backbones (Figure 4a and c). The layer organization is controlled predominantly by two types of C–H···O hydrogen bonds, differing by the oxygen atoms involved in these interactions. The carbonyl group oxygen atom interacts with hydrogen atoms of alkyl or aryl groups of the translated oxacyclophane molecules. The respective geometries of these C–H···O hydrogen bonds are C···O, H···O, C–H···O, 3.23, 2.54 Å, 129° in **11**, and 3.39, 2.47 Å, 170° in **13**, respectively. These interactions are responsible for the tapes running along *b* direction both in **11** and **13**. The OCH_2 groups form the weaker C–H···O bonds that are in the *bc* plane and close the layered $R_2^2(8)$ rings that are built on the methylene group hydrogen atom and the neighboring oxygen atom.[18] These hydrogen bonds have C···O, H···O distances and CH···O angles equal to 3.46, 2.62 Å, 146° in **11** and 3.60, 2.71 Å, 153° in **13**. The packing of the layers is governed by the π–π stacking interactions between the partially overlapping fluorenone units. The interlayer separation is 3.37 Å in **11** and 3.53 Å in **13**. The molecules of **12** are packed to form the chevron-like sheets (Figure 4b). The adjacent rows are oriented to optimize T-type edge-to-face interactions between the aromatic components with the dihedral angle of 103° between the planes of inclined fluorenone moieties.[19] These sheets are also interconnected into a three-dimensional grid through C–H···O hydrogen bonds, with respective geometries of C···O, H···O, CH···O, 3.55, 2.59 Å, 170° and 3.42, 2.49 Å, 160°.

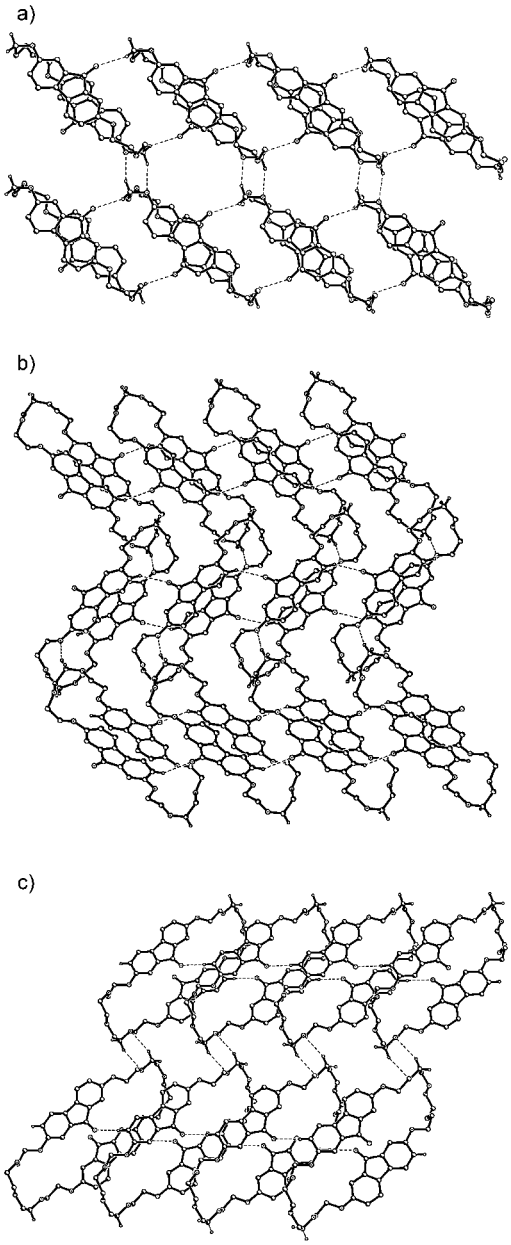

Figure 4. The part of one of the sheets sustained by the hydrogen bonds presented in the solid-state structure of the oxacyclophanes a) **11**, b) **12**, and c) **13**.

Complexation studies: A very low solubility of the oxacyclophanes **11**–**13** in usual organic solvents restricts application of NMR spectroscopy for investigations of their complexation in solutions. The [D_6]DMSO was the only solvent suitable for NMR experiments. Because this medium weakens or suppresses the formation of complexes,[20] we did not observe pronounced induced changes in the chemical shifts of the protons of the hosts **11**–**13** or the guest **18** in NMR spectra for the samples of their mixtures. A convenient way to explore the binding ability of macrocyclic hosts is mass spectrometry, which gives the opportunity to study host–guest chemistry as a purely bimolecular interaction in the absence of solvents and other interfering species.[21] Therefore, the complexation of the oxacyclophanes **11**–**13** with 1,1′-dimethyl-4,4′-bipyridinium bis(hexafluorophosphate) (**18**; Figure 2) in the gas phase was analyzed by fast atom bombardment mass spectrometry (FAB-MS). The separate samples of equimolar amounts of paraquat **18** and compounds **11**, **12**, or **13** dissolved in a DMF/*m*-nitrobenzyl alcohol mixture (1:1) were subjected to FAB-MS analysis. In the cases of both **12** and **13**, peaks were observed in the mass spectra that correspond to the loss of one and two PF_6^- counterions from the formed 1:1 complexes (Table 2). This fragmentation pattern has been observed in many pseudorotaxanes and catenanes derived from paraquat derivatives.[6b,22] However, no signal was observed which indicated that a complex had been formed with compound **11**.

Table 2. FAB-MS data for the complexes of **11**–**13** with **18**·2PF_6.

	$[M]^+$[a]	$[M-PF_6]^+$[b]	$[M-2PF_6]^+$[b]	Host[b,c]
11	[1040]	–	–	565 (100)
12	[1128]	983 (5)	838 (2)	653 (100)
13	[1216]	1071 (7)	926 (2)	741 (100)

[a] The peaks corresponding to the molecular ion of the complexes were not observed. [b] The peaks intensities are shown in parentheses. [c] Peaks corresponding to the protonated oxacyclophanes.

Inspection of CPK models revealed that the paraquat **18** could be easily accommodated inside the macrocycles **12** and **13**, but also that there are significant steric restrictions on its penetration into the cavity of the macrocycle **11**. Further computer modeling (a Monte Carlo conformational search in conjunction with the MMFF force field; semiempirical AM1 single-point energy calculations)[23] indicated that in the most stable structures of the complexes **12·18** and **13·18** the oxacyclophanes possess *anti*-conformations. The macrocycles cavities are tightly filled by compound **18**, which is located at the averaged distances of 4.0 and 3.9 Å between the centroids of the fluorenone units and paraquat for the **12·18** and **13·18**, respectively. These distances are appropriate for π–π stacking interactions (Figure 5b and c). The oxygen atoms of the carbonyl groups are directed towards the paraquat **18** at averaged distances from its centroid of 3.8 and 3.7 Å for the complexes **12·18** and **13·18**, respectively. This immediately indicates the considerable dipole–charge interactions between the carbonyl groups of the fluorenone moieties and the paraquat that are undoubtedly an important stabilization component of the complexes. The structures of the complexes **12·18** and **13·18** are additionally stabilized by C−H···O interactions between the acidic hydrogen atoms of paraquat methyl groups and the oxygen atoms of the polyether loops of the oxacyclophanes **12** and **13**. In a general way the calculated structure of the **12·18** is similar to that described for the pseudorotaxane-like complexes of paraquat with bisarylene crown ethers in the solid state, for example with bis-*p*-phenylene[34]crown-10,[6b] while the **13·18** has a "hot dog" structure.[24] In contrast, only the external complex of the *syn*-conformer of oxacyclophane **11** with the paraquat **18** was found in the energy window of 10 kcal mol^{-1}. The most stable structure of the **11·18** is held together by electrostatic interactions between two carbonyl groups of **11** and one of the nitrogen atoms of **18** (C=O···N$^+$ distances are 3.1 and 3.3 Å) and by hydrogen bonding involving the hydrogen atoms of the bipyridine and the ether oxygen atoms of the macrocycle (Figure 5a). The calculated stabilization energy values of the complexes **11·18**, **12·18**, and **13·18** are 31.9, 33.1, and 43.8 kcal mol^{-1}, respectively. The larger stabilization energy of the **13·18** complex with respect to the **12·18** is in agreement with the relative intensities of $[M-PF_6]^+$ peaks in their FAB mass spectra. Nevertheless, the complex **11·18** is not formed despite the fact that its stabilization energy in vacuo is similar to that of the **12·18**. Many publications demonstrate that in FABMS the signals are generated by direct desorption of the complex ions preformed in the condensed phase.[21] The formation of host–guest complexes in the condensed phase implies the solvation of both counterparts and hence the possible modification of a variety of noncovalent interactions between them. Therefore, the calculated values of the stabilization energy of the complexes do not necessarily reflect complexation in solution closely enough. The protic and highly polar DMF/*m*-nitrobenzyl alcohol matrix used in our experiments is a medium in which hydrogen bonds and electrostatic interactions responsible for complex formation become weak or even destroyed. Probably the competing salvation effect is strong enough to prevent formation of an external complex of the oxacyclophane **11**, while the formation of the less-solvated inclusion complexes of the oxacyclophanes **12** and **13** are permitted.

Conclusion

We have reported the synthesis of a new family of macrocyclic receptors, bis(oxofluorenediyl)oxacyclophanes, containing two fragments of 2,7-dioxyfluorenone bridged by the di-, tri-, and tetraethylene glycol units. An essential feature of these oxacyclophanes is the presence within the macrocyclic framework of highly polarized, π-electron-rich, extended aromatic systems of the fluorenone that can stabilize the complexes as a result of electrostatic interactions and hydrogen

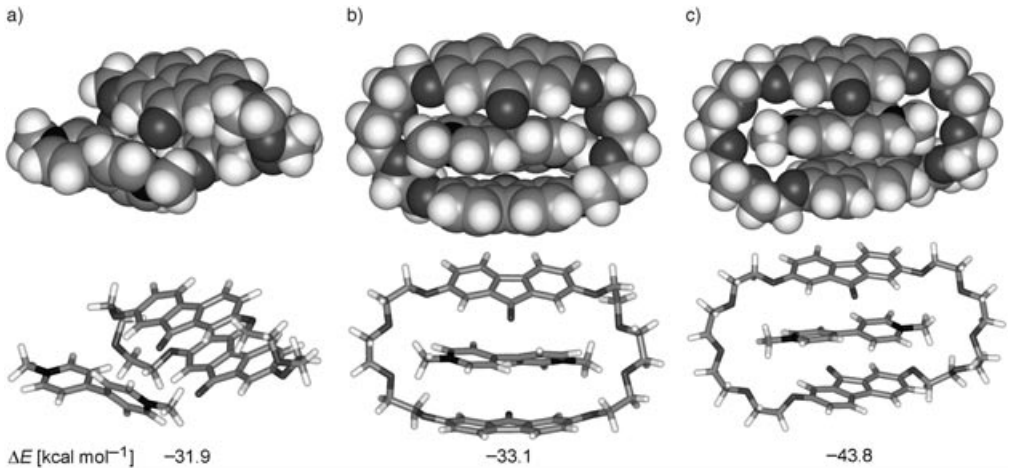

Figure 5. Calculated structures and stabilization energy (ΔE) of the complexes of paraquat **18** with oxacyclophanes a) **11**, b) **12**, and c) **13**. The ΔE values are the difference between the energies of the global minima of the complexes $E_{complex}$ and the energies of the global minima of the free host and guest E_{host} and E_{guest}, respectively ($\Delta E = E_{complex} - E_{host} - E_{guest}$).

bond formation with the substrate. These interactions are often the dominating factors of molecular recognition and self-assembly of supramolecular systems. As a result they make bis(oxofluorenediyl)oxacyclophanes attractive macrocyclic receptors for ionic and neutral species and as components in supramolecular synthesis. Future work will focus on exploring the ability of this macrocycle to act as a host for organic guest molecules.

Experimental Section

General: Chlorohydrins (**2**) and (**3**), and triethylene glycol bistosylate are commercially available and were used as received. 2,7-Dioxy-9*H*-fluoren-9-one (**1**),[8] chlorohydrin (**4**),[25] 2,7-dimethoxy-9*H*-fluoren-9-one (**17**)[26] and 2-hydroxy-7-methoxy-9*H*-fluoren-9-one[27] were prepared as described. Thin-layer chromatography (TLC) was carried out on aluminum sheets coated with silica gel 60F (Merck 5554). The plates were inspected by UV light and, if required, developed in I_2 vapor. Column chromatography was carried out by using silica gel (Acros 0.060–0.200 mm). Melting points were determined in open capillaries and are uncorrected. All ^{1}H and ^{13}C NMR spectra were recorded on Varian VXR-300 (300 MHz and 75.5 MHz, respectively) spectrometer. All chemical shifts are quoted in ppm on the δ scale with TMS or residual solvent as an internal standard. The coupling constants are expressed in Hz. Infrared spectra were recorded on a Specord 75 IR instrument. Electronic absorption spectra were obtained on a Specord M 40 spectrophotometer in the 200–900 nm range, in quartz cells with 1 cm path length. Electron impact (EI) mass spectra were recorded on a MX-1321 spectrometer at 70 eV. Fast atom bombardment (FAB) mass spectrometry was performed on a VG 7070 EQ mass spectrometer, equipped with a xenon primary atom beam, and an *m*-nitrobenzyl alcohol matrix was utilized.

General procedure for the preparation of the diols 5–7: Bisphenol **1** (16.98 g, 80 mmol) was added to suspension of freshly ground K_2CO_3 (66.34 g, 480 mmol) and NaI (24.00 g, 160 mmol) in dry DMF (400 mL) under argon. After stirring for 1 h at 60 °C, chlorohydrin **2**, **3**, or **4** (240 mmol) was added and the temperature was raised to 80 °C. Stirring and heating were continued for 35 h. After cooling to room temperature, the reaction mixture was filtered and the residue was washed with DMF (50 mL). The filtrate was evaporated to dryness in vacuo. The residue was dissolved in chloroform, and the solution was washed consequently with 5 % aqueous NaOH, water and brine, dried over $MgSO_4$, and evaporated in vacuo. The residue was purified by recrystallization from isopropyl alcohol for **5** and **6**, and from ethanol/diethyl ether for **7**.

2,7-Bis[2-(2-hydroxyethoxy)ethoxy]-9*H*-fluoren-9-one (5): Red solid (24.21 g, 78 %); m.p. 117–119 °C; ^{1}H NMR ($CDCl_3$): δ = 1.97 (brs, 2H), 3.65–3.72 (m, 4H), 3.74–3.82 (m, 4H), 3.84–3.92 (m, 4H), 4.14–4.21 (m, 4H) 6.97 (dd, J = 2, 8 Hz, 2H), 7.17 (d, J = 2 Hz, 2H), 7.29 ppm (d, J = 8 Hz, 2H); IR (KBr): $\tilde{\nu}$ = 1700 cm^{-1} (C=O); UV/Vis (CH_3OH): $\lambda_{max}(\varepsilon)$ = 270 (100000), 469 (269); MS (EI): *m*/*z* (%): 388 (44) $[M]^+$, 300 (7), 212 (35), 45 (100); elemental analysis calcd (%) for $C_{21}H_{24}O_7$ (388.4): C 64.94, H 6.23; found: C 65.19, H 6.29.

2,7-Bis{2-[2-(2-hydroxyethoxy)ethoxy]ethoxy}-9*H*-fluoren-9-one (6): Red solid (29.32 g, 77 %); m.p. 91–92 °C; ^{1}H NMR ($CDCl_3$): δ = 2.18 (brs, 2H), 3.63 (t, J = 4 Hz, 4H), 3.68–3.82 (m, 12H), 3.87 (t, J = 4 Hz, 4H), 4.17 (t, J = 4 Hz, 4H), 6.97 (dd, J = 2, 8 Hz, 2H), 7.17 (d, J = 2 Hz, 2H), 7.28 ppm (d, J = 8 Hz, 2H); IR (KBr): $\tilde{\nu}$ = 1700 cm^{-1} (C=O); UV/Vis (CH_3OH): $\lambda_{max}(\varepsilon)$ = 270 (88261), 473 nm (336); MS (EI): *m*/*z* (%): 476 (41) $[M]^+$, 432 (3), 344 (3), 212 (11), 45 (100); elemental analysis calcd (%) for $C_{25}H_{32}O_9$ (476.5): C 63.01, H 6.77; found: C 62.82, H 6.65.

2,7-Bis{2-[2-[2-(2-hydroxyethoxy)ethoxy]ethoxy}ethoxy}-9*H*-fluoren-9-one (7): Orange solid (36.09 g, 80 %); m.p. 61–63 °C; ^{1}H NMR ($CDCl_3$): δ = 2.07 (brs, 2H), 3.61 (t, J = 4 Hz, 4H), 3.65–3.77 (m, 20H), 4.17 (t, J = 4 Hz, 4H), 4.28 (t, J = 4 Hz, 4H), 6.97 (dd, J = 2, 8 Hz, 2H), 7.17 (d, J = 2 Hz, 2H), 7.28 ppm (d, J = 8 Hz, 2H); IR (KBr): $\tilde{\nu}$ = 1700 cm^{-1} (C=O); UV/Vis (CH_3OH): $\lambda_{max}(\varepsilon)$ = 270 (77664), 300 (6725), 312 (6287), 469 nm (273); MS (EI): *m*/*z* (%): 564 (14) $[M]^+$, 388 (2), 212 (10), 45 (100); elemental analysis calcd (%) for $C_{29}H_{40}O_{11}$ (564.6): C 61.69, H 7.14; found: C 61.87, H 6.94.

General procedure for the preparation of the bistosylates 8–10: A solution of *p*-toluenesulfonyl chloride (14.30 g, 75 mmol) in dry dioxane (30 mL) was added dropwise to solution of **5–7** (30 mmol) and triethylamine (9.11 g, 90 mmol) in chloroform over 2 h at 0–5 °C. The solution was allowed to warm to RT and stirring was continued for 30 h. An equal volume of chloroform was added to the slurry and the mixture was successively washed with 5 % aqueous HCl, 10 % aqueous ammonia, water, and brine, and dried over $MgSO_4$. After evaporation of the solvent, crude product was extracted with hot isopropyl alcohol. Pure bistosylates were isolated on cooling solution.

2-{2-{{7-{2-{2-{[(4-methylphenyl)sulfonyl]oxy}ethoxy}ethoxy}-9-oxo-9*H*-fluoren-2-yl}oxy}ethoxy}ethyl 4-methylbenzenesulfonate (8): Orange-red solid (18.37 g, 88 %); m.p. 110–112 °C; ^{1}H NMR ($CDCl_3$): δ = 2.42 (s, 6H), 3.73–3.83 (m, 8H), 4.07 (t, J = 4 Hz, 4H), 4.21 (t, J = 4 Hz, 4H), 6.95 (dd, J = 2, 8 Hz, 2H), 7.12 (d, J = 2 Hz, 2H), 7.27–7.36 (m, 6H), 7.80 ppm (d, J = 8 Hz, 4H); IR (KBr): $\tilde{\nu}$ = 1700 cm^{-1} (C=O); UV/Vis (dioxane): $\lambda_{max}(\varepsilon)$ = 272 (91636), 301 (7958), 314 (7615), 464 nm (373); MS (EI): *m*/*z* (%): 696 (5) $[M]^+$, 524 (26), 497 (7), 282 (10), 212 (31); elemental analysis calcd (%) for $C_{35}H_{36}O_{11}S_2$ (696.8): C 60.33, H 5.21; found: C 60.47, H 5.41.

2-{2-{2-{{7-{2-{{-{2-{[(4-methylphenyl)sulfonyl]oxy}ethoxy}ethoxy}ethoxy}-9-oxo-9*H*-fluoren-2-yl}oxy}ethoxy}ethoxy}ethyl 4-methylbenzenesulfonate (9): Orange solid (19.75 g, 84 %); m.p. 68–70 °C; ^{1}H NMR ($CDCl_3$): δ = 2.43 (s, 6H), 3.57–3.75 (m, 12H), 3.79–3.87 (m, 4H), 4.08–4.21 (m, 8H), 6.97 (dd, J = 2, 8 Hz, 2H), 7.15 (d, J = 2 Hz, 2H), 7.29 (d, J = 8 Hz, 2H), 7.33 (d, J = 8 Hz, 4H), 7.80 ppm (d, J = 8 Hz, 4H); IR (KBr): $\tilde{\nu}$ = 1700 cm^{-1} (C=O); UV/Vis (dioxane): $\lambda_{max}(\varepsilon)$ = 225 (52742), 272 (139197), 301 (12700), 314 (12173), 469 nm (518); MS (FAB): *m*/*z* (%): 785 (100) $[M+H]^+$; elemental analysis calcd (%) for $C_{39}H_{44}O_{13}S_2$ (784.9): C 59.68, H 5.65; found: C 59.56, H 5.47.

2-{2-{2-{2-{{7-{2-{2-{2-{2-{[(4-methylphenyl)sulfonyl]oxy}ethoxy}ethoxy}-ethoxy}ethoxy}-9-oxo-9*H*-fluoren-2-yl}oxy}ethoxy}ethoxy}ethoxy}ethyl 4-methylbenzenesulfonate (10): Dark red viscous oil, solidified on standing (18.31 g, 70 %); ^{1}H NMR ($CDCl_3$): δ = 2.43 (s, 6H), 3.60 (s, 8H), 3.62–3.76 (m, 12H), 3.85 (t, J = 4 Hz, 4H), 4.11–4.20 (m, 8H), 6.97 (dd, J = 2, 8 Hz, 2H), 7.15 (d, J = 2 Hz, 2H), 7.28 (d, J = 8 Hz, 2H), 7.33 (d, J = 8 Hz, 4H), 7.79 ppm (d, J = 8 Hz, 4H); IR (KBr): $\tilde{\nu}$ = 1700 cm^{-1} (C=O); UV/Vis (dioxane): $\lambda_{max}(\varepsilon)$ = 229 (25270), 272 (90783), 302 (7635), 314 (7516), 464 nm (439); MS (FAB): *m*/*z* (%): 873 (100) $[M+H]^+$; elemental analysis calcd (%) for $C_{43}H_{52}O_{15}S_2$ (872.9): C 59.16, H 6.00; found: C 58.98, H 5.83.

General procedure for the preparation of the oxacyclophanes 11–13: A solution of **1** (2.12 g, 10 mmol) and the appropriate bistosylate **8–10** (10 mmol) in dry DMF (400 mL) was added dropwise over 10 h to a stirred suspension of K_2CO_3 (5.52 g, 40 mmol) in DMF (600 mL) under argon at 80 °C; heating was then maintained for a further 40 h. The reaction mixture was filtered, and the filtrate was evaporated to dryness in vacuo. The residue and solid obtained after the first filtration were combined, washed with cold methanol, and filtered. The air-dried solid was extracted with toluene by using a Soxhlet extractor for 40 h. The toluene extract was filtered and the solid residue was extracted with hot toluene several times until complete extraction of the product. The solvent was removed from the combined toluene extracts under reduced pressure, the residue washed with a small amount of acetone and then subjected to column chromatography (SiO_2, $CHCl_3$/MeOH, 100:1), to afford pure oxacyclophanes.

Oxacyclophane 11: Dark red crystals (2.98 g, 53 %); m.p. 296—298 °C (decomp); ^{1}H NMR ([D$_6$]DMSO): δ = 3.81 (t, J = 3 Hz, 8H), 4.09 (t, J = 3 Hz, 8H), 6.66 (brs, 4H), 6.84 (dd, J = 2, 8 Hz, 4H), 7.16 ppm (d, J = 8 Hz, 4H); ^{13}C NMR (CF_3COOD): δ = 69.9, 71.9, 115.8, 123.1, 123.6, 137.5, 140.7, 160.9, 200.3 ppm; IR (KBr): $\tilde{\nu}$ = 1700 cm^{-1} (C=O); UV/Vis (dioxane): $\lambda_{max}(\varepsilon)$ = 264 (119785), 302 (11201), 314 (10843), 473 nm (507); MS (EI): *m*/*z* (%): 564 (100) $[M]^+$, 282 (7), 239 (8), 212 (11); elemental analysis calcd (%) for $C_{34}H_{28}O_8$ (564.6): C 72.33, H 5.00; found: C 72.26, H 5.25.

Oxacyclophane 12: Red crystals (1.76 g, 27%); m.p. 197—199°C; ^{1}H NMR ([D$_6$]DMSO): δ=3.65 (s, 8H), 3.75 (t, J=4 Hz, 8H), 4.04 (t, J=4 Hz, 8H), 6.80 (br s, 4H), 6.82 (br d, J=8 Hz, 4H), 7.11 ppm (d, J=8 Hz, 4H); ^{13}C NMR (CF_3COOD): δ=67.6, 70.5, 71.2, 111.1, 121.8, 123.0, 135.7, 139.6, 159.4, 198.8 ppm; IR (KBr): $\tilde{\nu}$= 1700 cm^{-1} (C=O); UV/Vis (dioxane): $\lambda_{max}(\varepsilon)$=264 (123029), 302 (11591), 314 (10895), 470 nm (459); MS (EI): m/z (%): 652 (100) $[M]^+$, 580 (16), 326 (14), 212 (18); elemental analysis calcd (%) for $C_{38}H_{36}O_{10}$ (652.7): C 69.93, H 5.56; found: C 69.77, H 5.69.

Oxacyclophane 13: Orange crystals (2.22 g, 30%); m.p. 176—177°C; ^{1}H NMR ([D$_6$]DMSO): δ=3.59 (s, 8H), 3.75 (br s, 8H), 3.99 (br s, 8H), 6.84 (br s, 8H), 7.18 ppm (d, J=8 Hz, 4H); ^{13}C NMR ($CDCl_3$): δ=68.1, 69.7, 70.8, 71.1, 110.0, 120.4, 120.7, 135.8, 137.4, 159.1, 193.2 ppm; IR (KBr): $\tilde{\nu}$= 1700 cm^{-1} (C=O); UV/Vis (dioxane): $\lambda_{max}(\varepsilon)$=263 (134464), 270 (119107), 302 (12685), 314 (11934), 468 nm (576); MS (EI): m/z (%): 740 (100) $[M]^+$, 369 (5), 238 (17), 212 (21); elemental analysis calcd (%) for $C_{42}H_{44}O_{12}$ (740.8): C 68.10, H 5.99; found: C 68.34, H 6.22.

Table 3. Crystal data, data collection, and refinement parameters of oxacyclophanes **11**, **12**, and **13**.

	11	**12**	**13**
formula	$C_{34}H_{28}O_8$	$C_{38}H_{36}O_{10}$	$C_{42}H_{44}O_{12}$
M_r [g mol^{-1}]	564.56	652.67	740.77
dimensions [mm]	0.36×0.35×0.12	0.35×0.18×0.05	0.20×0.15×0.04
T [K]	293(2)	293(2)	293(2)
crystal system	triclinic	monoclinic	triclinic
space group	$P\bar{1}$	$P2_1/c$	$P\bar{1}$
a [Å]	7.933(2)	8.372(2)	8.009(1)
b [Å]	8.747(2)	23.230(4)	8.531(1)
c [Å]	11.170(2)	8.660(2)	14.059(3)
α [°]	94.04(2)	90.0	102.33(3)
β [°]	109.24(2)	113.53(2)	99.68(3)
γ [°]	112.12(3)	90.0	91.39(2)
V [Å^3]	661.0(3)	1544.2(6)	923.3(3)
Z	1	2	1
ρ_{calc} [g cm^{-3}]	1.418	1.404	1.332
μ [cm^{-1}]	1.01	1.02	0.98
F(000)	296	688	392
θ range [°]	2.0–26.4	2.7–27.8	2.5–25.3
index range (h,k,l)	±9, 10, 13	±10, 29, 11	±9, 10, 16
reflns collected	8319	11986	8681
independent reflns	2642	3422	3257
reflns observed [$I>2\sigma(I)$]	1399	1468	1707
parameters	190	218	245
R_1 [$I>2\sigma(I)$]	0.0496	0.0546	0.0512
wR_2 (F^2)	0.0999	0.1237	0.1052
goodness-of-fit	0.930	0.819	0.955
$\Delta\rho_{max}$ [e Å^{-3}]	0.162	0.280	0.200
$\Delta\rho_{min}$ [e Å^{-3}]	−0.163	−0.306	−0.193

Compound 15: A solution of 2-hydroxy-7-methoxy-9*H*-fluoren-9-one (2.40 g, 10.6 mmol) in dry DMF (20 mL) was added to suspension of freshly ground K_2CO_3 (2.92 g, 21.2 mmol) in dry DMF (20 mL) under argon. After stirring at 60°C for 20 min, a solution of triethyleneglycol bistosylate (2.29 g, 5 mmol) in dry DMF (20 mL) was added to the mixture over 30 min, and the temperature was raised to 80°C. Stirring and heating were continued for 12 h. After cooling to room temperature, the reaction mixture was filtered and the residue was washed with a small amount of DMF. The filtrate was evaporated in vacuo, the residue was dissolved in chloroform, and the solution was washed consequently with 5% aqueous NaOH, water, and brine, dried over $MgSO_4$, and evaporated at reduced pressure. The residue was subjected to column chromatography (SiO_2, $CHCl_3$/MeOH, 100:1) to afford pure **15** as bright red crystals (1.66 g, 58%). M.p. 150–150.5°C; ^{1}H NMR ($CDCl_3$): δ=3.76 (s, 4H), 3.82 (s, 6H), 3.85–3.90 (m, 4H), 4.11–4.17 (m, 4H), 6.87–6.96 (m, 4H), 7.10–7.14 (m, 4H), 7.21–7.26 ppm (m, 4H); MS (EI): m/z (%): 566 (100) $[M]^+$, 340 (17), 283 (16), 253 (37), 226 (76), 211 (31); elemental analysis calcd (%) for $C_{34}H_{30}O_8$ (566.6): C 72.07, H 5.34; found: C 72,13, H 5.38.

X-ray crystallographic data for 11, 12, and 13: Table 3 provides a summary of the crystallographic data for compounds **11**–**13**. Data were collected at a room temperature on a Nonius Kappa CCD diffractometer equipped with graphite monochromated $Mo_{K\alpha}$ radiation by using φ–ω scans with a sample-to-detector distance of 29 mm. Unit cell parameters were obtained and refined using the whole data set. Frames were integrated and corrected for Lorentz and polarization effects using DENZO.[28] The scaling and global refinement of crystal parameters were performed by SCALEPACK.[28] The structure solution and refinement proceeded similarly for all structures using SHELX97 program package.[29] All structures were solved by direct methods (SHELXS-97) and refined on F^2 by full-matrix least-squares techniques (SHELXL-97). The geometrically constrained hydrogen atoms were placed in calculated positions with isotropic temperature factors (1.2 times the carbon temperature factor) and refined as riding atoms.

CCDC 239347, 204895, and 239346 contain the supplementary crystallographic data for this paper. These data can be obtained free of charge via www.ccdc.cam.ac.uk/conts/retrieving.html (or from the Cambridge Crystallographic Data Centre, 12, Union Road, Cambridge CB2 1EZ, UK; fax: (+44) 1223-336-033; or deposit@ccdc.cam.ac.uk).

Acknowledgement

The diffraction data were collected at the Department of Chemistry, Technion, The Haifa, through the cooperation of Professor Menahem Kaftory whom we would like to acknowledge.

[1] a) D. J. Cram, J. M. Cram, *Container Molecules and their Guests*, The Royal Society of Chemistry, Cambridge, **1994**; b) F. Diederich, *Cyclophanes*, The Royal Society of Chemistry, Cambridge, **1991**; c) F. Vögtle, *Cyclophane Chemistry*, Wiley, Chichester, **1993**; d) S. Apel, M. Lennartz, L. R. Nassimbeni, E. Weber, *Chem. Eur. J.* **2002**, *8*, 3678–3686; e) C. E. O. Roesky, E. Weber, T. Rambusch, H. Stephan, K. Gloe, M. Czugler, *Chem. Eur. J.* **2003**, *9*, 1104–1112; f) P. Sarri, F. Venturi, F. Cuda, S. Roelens, *J. Org. Chem.* **2004**, *69*, 3654–3661; g) H.-J. Schneider, A. Yatsimirski, *Principles in Supramolecular Chemistry*, Wiley, Chichester, **2000**.

[2] a) S. Inokuma, S. Sakaki, J. Nishimura, *Top. Curr. Chem.* **1994**, *172*, 87–118; b) S. Tsuzuki, H. Houjou, Y. Nagawa, M. Goto, K. Hiratani, *J. Am. Chem. Soc.* **2001**, *123*, 4255–4258; c) J. H. Hartley, T. D. James, C. J. Ward, *J. Chem. Soc. Perkin Trans. 1* **2000**, 3155–3184; d) J. W. Steed, J. L. Atwood, *Supramolecular Chemistry*, Wiley, Chichester, **2000**.

[3] For papers and reviews on these noncovalent interactions, see: a) G. R. Desiraju, *Acc. Chem. Res.* **2002**, *35*, 565–573; b) F. M. Raymo, M. D. Bartberger, K. N. Houk, J. F. Stoddart, *J. Am. Chem. Soc.* **2001**, *123*, 9264–9267; c) C. A. Hunter, K. R. Lawson, J. Perkins, J. Urch, *J. Chem. Soc. Perkin Trans. 2* **2001**, 651–669; d) E. A.

Meyer, R. K. Castellano, F. Diederich, *Angew. Chem.*, **2003**, *115*, 1244–1287; *Angew. Chem. Int. Ed.* **2003**, *42*, 1210–1250; e) M. Nishio, Y. Umezawa, M. Hirota, Y. Takeuchi, *The CH···π Interaction*, Wiley-VCH, New York, **1998**; f) G. Chessari, C. A. Hunter, C. M. R. Low, M. J. Packer, J. G. Vinter, C. Zonta, *Chem. Eur. J.* **2002**, *8*, 2860–2867; g) M. Blanco, M. C. Jiménez, J.-C. Chambron, V. Heitz, M. Linke, J.-P. Sauvage, *Chem. Soc. Rev.* **1999**, *28*, 293–305; h) T. J. Hubin, D. H. Busch, *Coord. Chem. Rev.* **2000**, *200–202*, 5–52; i) G. W. Gokel, S. L. De Wall, E. S. Meadows, *Eur. J. Org. Chem.* **2000**, 2967–2978.

[4] K. Müller-Dethlefs, P. Hobza, *Chem. Rev.* **2000**, *100*, 143–167, and references therein.

[5] a) F. Toda, *Acc. Chem. Res.* **1995**, *28*, 480–486; b) E. Weber, R. Haase, R. Pollex, M. Czugler, *J. Prakt. Chem.* **1999**, *341*, 274–283; c) E. Weber, C. Helbig, W. Seichter, M. Czugler, *J. Inclusion Phenom.* **2002**, *43*, 239–246.

[6] a) B. L. Allwood, N. Spencer, H. Shahriari-Zavareh, J. F. Stoddart, D. J. Williams, *J. Chem. Soc. Chem. Commun.* **1987**, 1058–1060; b) P. L. Anelli, P. R. Ashton, R. Ballardini, V. Balzani, M. Delgado, M. T. Gandolfi, T. T. Goodnov, A. E. Kaifer, D. Philp, M. Pietraszkiewicz, L. Prodi, M. V. Reddington, A. M. Z. Slawin, N. Spencer, J. F. Stoddart, C. Vicent, D. J. Williams, *J. Am. Chem. Soc.* **1992**, *114*, 193–218, and references therein.

[7] a) J. F. Stoddart, H.-R. Tseng, *Proc. Natl. Acad. Sci. USA* **2002**, *99*, 4797–4800; b) *Molecular Catenanes, Rotaxanes and Knots* (Eds.: J.-P. Sauvage, C. O. Dietrich-Buchecker), Wiley-VCH, Weinheim, **1999**; c) D. B. Amabilino, J. F. Stoddart, *Chem. Rev.* **1995**, *95*, 2725–2828; d) D. Philp, J. F. Stoddart, *Angew. Chem.* **1996**, *108*, 1242–1286; *Angew. Chem. Int. Ed. Engl.* **1996**, *35*, 1154–1196; e) F. M. Raymo, J. F. Stoddart, *Chem. Rev.* **1999**, *99*, 16431663; f) C. A. Schalley, K. Beizai, F. Vögtle, *Acc. Chem. Res.* **2001**, *34*, 465476; g) X.-Y. Li, J. Illigen, M. Nieger, S. Michel, C. A. Schalley, *Chem. Eur. J.* **2003**, *9*, 1332–1347; h) H. W. Gibson in *Large Ring Molecules* (Ed.: J. A. Semlyen), Wiley, New York, **1996**, pp. 191–262; i) A. L. Hubbard, G. J. E. Davidson, R. H. Patel, J. A. Wisner, S. J. Loeb, *Chem. Commun.* **2004**, 138–139.

[8] E. R. Andrews, R. W. Fleming, J. M. Grisar, J. C. Kihm, D. L. Wenstrup, G. D. Mayer, *J. Med. Chem.* **1974**, *17*, 882–886.

[9] N. G. Lukyanenko, T. I. Kirichenko, A. Yu. Lyapunov, T. Yu. Bogaschenko, V. N. Pastushok, Yu. A. Simonov, M. S. Fonari, M. M. Botoshansky, *Tetrahedron Lett.* **2003**, *44*, 7373–7376.

[10] For papers and reviews on the cesium effect, see: a) A. Ostrowicki, E. Koepp, F. Vögtle, *Top. Curr. Chem.* **1991**, *161*, 37–58; b) D. A. Laidler, J. F. Stoddart in *The Chemistry of Ethers, Crown Ethers, Hydroxyl Groups and Their Sulphur Analogues*, *Vol. 1* (Ed.: S. Patai), Wiley, Chichester, **1980**, pp. 1–58; c) G. W. Gokel, B. J. Garcia, *Tetrahedron Lett.* **1977**, *18*, 317–320; d) G. Dijkstra, W. H. Kruizinga, R. M. Kellogg, *J. Org. Chem.* **1987**, *52*, 4230–4237.

[11] Spartan 02 (Version 1.0.2, 2002), Wavefunction, Inc., Irvine, CA.

[12] A. M. Z. Slawin, N. Spencer, J. F. Stoddart, D. J. Williams, *J. Chem. Soc. Chem. Commun.* **1987**, 1070–1072.

[13] W. Zhang, X. Shao, L. Yang, Z.- L. Liu, Y. L. Chow, *J. Chem. Soc. Perkin Trans. 2* **2002**, 1029–1033.

[14] G. Guinand, P. Marsau, H. Bouas-Laurent, A. Castellan, J.-P. Desvergne, M.-H. Riffaud, *Acta Crystallogr. Sect. C* **1986**, *42*, 835–838.

[15] Ya. Delaviz, J. S. Merola, M. A. G. Berg, H. W. Gibson, *J. Org. Chem.* **1995**, *60*, 516–522.

[16] a) N. K. Dalley, J. S. Smith, S. B. Larson, J. J. Christensen, R. M. Izatt, *J. Chem. Soc. Chem. Commun.* **1975**, 43–44; b) E. Maverick, P. Seiler, W. B. Schweizer, J. D. Dunitz, *Acta Crystallogr. Sect. B* **1980**, *36*, 615–620; c) C. L. Raston, P. J. Nichols, K. Baranyai, *Angew. Chem.* **2000**, *112*, 1913–1915; *Angew. Chem. Int. Ed.* **2000**, *39*, 1842–1845; d) K. Yamato, R. A. Bartsch, M. L. Dietz, R. D. Rogers, *Tetrahedron Lett.* **2002**, *43*, 2153–2156; e) K. Yamato, R. A. Bartsch, G. A. Broker, R. D. Rogers, M. L. Dietz, *Tetrahedron Lett.* **2002**, *43*, 5805–5808; f) V. Ch. Kravtsov, M. S. Fonari, M. J. Zaworotko, J. Lipkowski, *Acta Crystallogr. Sect. C* **2002**, *58*, o683–o684.

[17] The loops of the crown ether are described by the following sequences of *anti* (*a*), *cis* (*c*) and *gauche* (*g*) torsion angles in the independent part of the molecule, beginning from the bond involving the oxygen atom attached to the fluorenone unit, and the value of the torsion angle C_{aryl}-C_{aryl}-O-$C_{methylene}$, *a*-(165.7(2)), *g*-(−76.9(3)), *g*-(−65.4(2)), *a*-(158.4(2)), *g*-(−91.4(2)), *g*(75.3(3)), *a*-(−170.1(2)), *a*-(−172.4(2))° for **11**; *c*-(−8.3(4)), *a*-(172.6(2)), *g*-(63.9(3)), *a*-(−154.0(2)), *g*-(71.4(3)), *g*-(−91.0(3)), *a*-(166.3(2)), *g*-(−78.5(3)), *g*-(−60.7(3)), *a*-(175.6(2)), *c*-(12.1(3))° for **12**; and *c*-(2.6(4)), *a*-(−179.9(2)), *g*-(74.3(3)), *a*-(175.9(2)), *a*-(−170.5(2)), *g*-(71.1(3)), *a*-(−150.2(2)), *a*-(172.1(2)), *g*-(−72.2(3)), *g*-(80.3(3)), *a*-(165.3(2)), *g*-(71.1(3)), *a*-(−167.3(2)), *a*-(171.4(2))° for **13**.

[18] M. C. Etter, J. C. MacDonald, J. Bernstein, *Acta Crystallogr. Sect. B* **1990**, *46*, 256–262.

[19] a) W. B. Jennings, B. M. Farrell, J. F. Malone, *Acc. Chem. Res.* **2001**, *34*, 885–894; b) R. A. Bartsch, P. Kus, N. K. Dalley, X. Kou, *Tetrahedron Lett.* **2002**, *43*, 5017–5019; c) M. J. Cloninger, H. W. Whitlock, *J. Org. Chem.* **1998**, *63*, 6153–6159.

[20] P. R. Ashton, I. Baxter, M. C. T. Fyfe, F. M. Raymo, N. Spencer, J. F. Stoddart, A. J. P. White, D. J. Williams, *J. Am. Chem. Soc.* **1998**, *120*, 2297–2307.

[21] a) Marco Vincenti, *J. Mass. Spectrom.* **1995**, *30*, 925–939; b) C. A. Schalley, *Int. J. Mass Spectrom.* **2000**, *194*, 11–39, and references therein.

[22] a) M. Asakawa, P. R. Ashton, R. Ballardini, V. Balzani, M. Belohradsky, M. T. Gandolfi, O. Kocian, L. Prodi, F. M. Raymo, J. F. Stoddart, M. Venturi, *J. Am. Chem. Soc.* **1997**, *119*, 302–310; b) W. S. Bryant, J. W. Jones, P. E. Mason, I. Guzei, A. L. Rheingold, F. R. Fronczek, D. S. Nagvekar, H. W. Gibson, *Org. Lett.* **1999**, *1*, 1001–1004.

[23] Each complex and its two separate components were subjected individually to Monte Carlo conformational searches by employing the MMFF force field as implemented in Spartan 02 (Ref. [11]). The energy of each of the minimized structures was obtained by single-point AM1 semiempirical calculations. The stabilization energy (ΔE) of the complexes formed from host and guest was evaluated following equation: $\Delta E = E_{complex} - E_{host} - E_{guest}$.

[24] P. R. Ashton, M. C. T. Fyfe, M.-V. Martínez-Díaz, S. Menzer, C. Schiavo, J. F. Stoddart, A. J. P. White, D. J. Williams, *Chem. Eur. J.* **1998**, *4*, 1523–1534.

[25] D. B. Amabilino, P. R. Ashton, C. L. Brown, E. Córdova, L. A. Godínez, T. T. Goodnow, A. E. Kaifer, S. P. Newton, M. Pietraszkievicz, D. Philp, F. M. Raymo, A. S. Reder, M. T. Rutland, A. Slawin, N. Spenser, J. F. Stoddart, D. J. Williams, *J. Am. Chem. Soc.* **1995**, *117*, 1271–1293.

[26] N. A. Barnes, R. W. Faessinger, *J. Org. Chem.* **1961**, *26*, 4544–4548.

[27] J. A. McCubbin, X. Tong, R. Wang, Y. Zhao, V. Snieckus, R. P. Lemieux, *J. Am. Chem. Soc.* **2004**, *126*, 1161–1167.

[28] Z. Otwinowski, W. Minor, *Methods Enzymol.* **1996**, *276*, 307–326.

[29] G. M. Sheldrick, SHELXS97 and SHELXL97, University of Göttingen (Germany), **1997**.

Received: September 11, 2004
Published online: November 18, 2004